

3D list-mode reconstruction for SPECT

L Bouwens[§], R Van de Walle[§], H Gifford[‡], I Lemahieu[§] and R A Dierckx[†]

[§] ELIS Department, MEDISIP, IBITECH, Ghent University
Sint-Pietersnieuwstraat 41 B-9000 Ghent, Belgium

[†] Nuclear Medicine Dept., Ghent University Hospital
De Pintelaan 185 B-9000 Ghent, Belgium

[‡] University of Massachusetts Medical School, Division of Nuclear Medicine
55 Lake Ave. North, Worcester, MA, USA

Abstract— In previous work we developed a list-mode iterative reconstruction algorithm (LMIRA) for SPECT applied to two dimensional image reconstruction. In the 2D case we calculated the emission radiance distribution on the circular enclosure of the object. This part is the forward projection. In the backprojection we sampled the radiance on the intermediate layer using the geometric properties of the collimator. In 3D reconstruction we have to calculate the emission radiance distribution on the cylindrical enclosure. To characterize the radiance on the cylinder we need additional parameters to localize the position on the layer and the direction of the escaping photons, this results in a 4 dimensional function. The probabilities used in the LMIRA update equation are calculated from sampling the radiance with the cylindrical hole structure of the collimator.

Keywords— List-mode, reconstruction, iterative.

I. INTRODUCTION

In binned mode PET the acquired data is often rebinned to 2D information using single slice rebinning or for example Fourier rebinning. In Single Photon Emission Computed Tomography (SPECT) reconstruction it is also possible not to use the 3D information and perform a 2D slice by slice reconstruction using the 2D reconstruction methods. 3D list-mode reconstruction has previously been the subject of research in positron emission tomography (PET) [1] and Compton scatter imaging [2]. Fully 3D reconstruction is useful to incorporate the complete blurring model to be able to correct for the distance dependent resolution [3], which is a three dimensional effect. Recently we developed a 2D list-mode reconstruction method for SPECT applying a new projector backprojector pair. The list-mode reconstruction approach differs in several ways from the bin-mode methods. Acquiring the data in list-mode format, one can store the interaction location to a high degree of accuracy (2k by 2k for example) with greater efficiency than achievable with frame mode acquisition. The gantry angles do not have to be binned into predefined frames, but one can record the actual angle thereby removing the impact of angular blurring with continuous acquisition. The actual energy of the interaction can be recorded instead of attributing the event's energy to one of a limited number of pre-defined windows. It is obvious that when increasing the dimensionality in this way it is no longer possible to bin the data into a matrix. Finally, list mode can also store gating signals without the need for temporal framing of the data

before this information is completely available. The result is a significant increase in the fidelity of recording the projection data with list-mode acquisition, without a tremendous increase in storage space. In bin-mode acquisition of SPECT data the number of detector locations is predefined and rarely exceeds 256×256 detector bins acquired over 120 angular steps. This means data will be grouped together thereby losing detailed information. For each bin i it is possible to obtain the probability of the i -th outcome, given an emission at the j -th voxel within the object. When the number of possible detector bins is limited one can calculate and store the entire transition matrix, giving the relationship between the object space and the detector space. With this information the probability of detecting an emission from the j -th voxel can be calculated. To calculate the maximum likelihood solution to this probabilistic problem, iterative methods such as expectation maximization maximum likelihood (MLEM) [4][5] have been presented. In list-mode the set of possible outcomes is so large that few of the outcomes occur maximum more than once and most of them never occur at all. In binned format this would mean that most of the elements of the, very large, sinogram are zero. Therefore it is more efficient to acquire the detected events in a list, together with their detection parameters such as detector location, gantry angle, energy, time stamp, etc. Since it is no longer possible to store the transition matrix, it will be necessary to calculate the probabilities, used in the reconstruction algorithm, on the fly. In our previous work this was done using a new approach: the intermediate layer. In previous work we developed a list-mode iterative reconstruction algorithm (LMIRA) [6] for SPECT applied to two dimensional image reconstruction. This reconstruction method used the geometric collimator model to apply the resolution recovery in a single slice [7]. In this work we deploy a modification of the projector and backprojector to fit the three dimensional reconstruction problem. First we will explain the transition of the calculation of the emission radiance distribution from 2D to 3D. Secondly we detail the sampling of the obtained radiance distribution with the three dimensional collimator structure will be described. Finally we will present the 3D list-mode reconstruction algorithm.

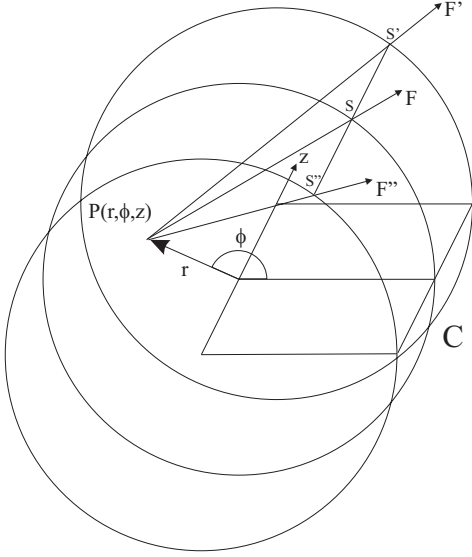


Fig. 1. Forward projection of the source distribution onto the intermediate layer.

II. METHOD

A. 3D emission radiance distribution

In 2D list-mode reconstruction a circular enclosure was used surrounding the object, called the intermediate layer. For the 3D problem, using for example a parallel hole or a fan beam collimator, a cylindrical enclosure will be best suited. For the imaging of small object with a pinhole or a cone beam collimator it may be that a sphere is more appropriate for this specific problem. In this work we discuss the case of a parallel hole collimator and thus use a cylindrical intermediate layer.

To calculate the radiance distribution on the intermediate layer an isotropic emission is generated at each point in the source distribution. For an isotropic emission generated at point $P(r, \phi, z)$ the contribution to the radiance in each point on the cylinder has to be calculated. For the location $S(\psi, z)$ on the cylinder, the emission from the source element P will be given by the vector $F_P(\psi, z, \theta, \kappa)$ (image 1). To obtain the radiance distribution from P at S one can use the known expression:

$$F_P(\psi, z, \theta, \kappa) = E_P \cdot \exp\left(-\int_P^S \mu(r, \Psi, z) \cdot ds\right), \quad (1)$$

With E_P the value of the source distribution at P , and $\mu(r, \Psi, z)$ the continuous attenuation coefficient distribution. The total emission radiance distribution $F(\psi, z, \theta, \kappa)$ in point S can be calculated by integration of the function F over the line through the object defined by S , θ and κ .

In the expression the parameters ψ and z indicate the location on the cylinder face. The parameters θ is the angle of the projection of F on the trans-axial slice through the source point P relative to horizontal x-axis and κ is the angle, obtained when projection F in the plane given by the axial line (z-axis) through the location point S and the normal vector N in S , relative to N . These parameters

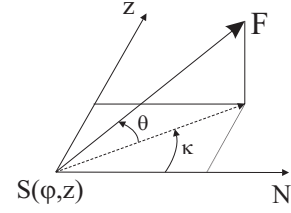


Fig. 2. Parameterizing the direction of the escape vector F .

give the direction of the escape vector F . To incorporate the detector response in the z direction we will need the additional parameter κ (image 2).

When projecting the source distribution to the intermediate layer it is possible to build in the following restriction. In the axial direction the projection can be limited by the known geometric parameters of the collimator. Since photons leaving the intermediate layer, with an angle κ greater than the acceptance angle of the collimator, will never be acceptable by the collimator holes, there is no need to calculate the projection beyond this point. In this way the axial projection can be restricted. The angle θ can not be restricted since the detector is rotating in this direction. Image 3 shows the emission radiance distribution for a point source. The right image is the surface plot of the left image. The top image is the complete distribution and the bottom image is the restricted radiance for a High Resolution parallel Hole (HR) Marconi collimator.

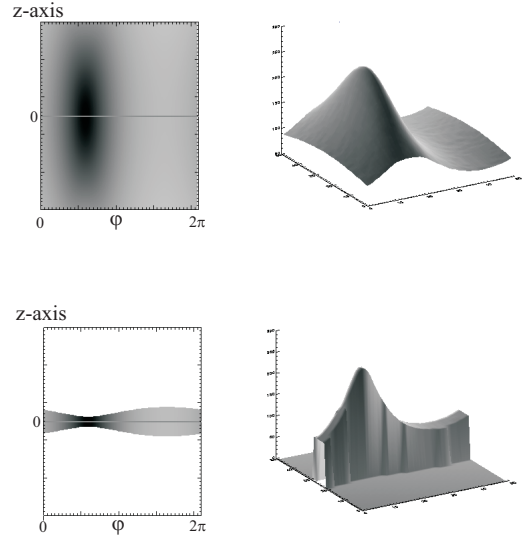


Fig. 3. Emission radiance distribution for a point source out of center. Top: complete radiance distribution. Bottom: radiance distribution restricted by the collimator axial acceptance angle.

B. Sampling the radiance distribution with a collimated detector

Consider data acquired from an object into list-mode information with the following parameters: axial location of incidence a , trans-axial location t and gantry angle δ . The collimator discussed primarily in this paper is a parallel

hole collimator. For each single list-mode event n in the reconstruction we place a collimator hole over the center of the detector location (a, t) . From the bottom area of the collimator hole towards the intermediate layer, (i.e. the cylinder shown in figure 1), we will see a fraction of the cylinder. Lines drawn from the outermost parts of the collimator hole, over the edges of the collimator septa, to the cylinder restrict the solid angle seen (figure 3).

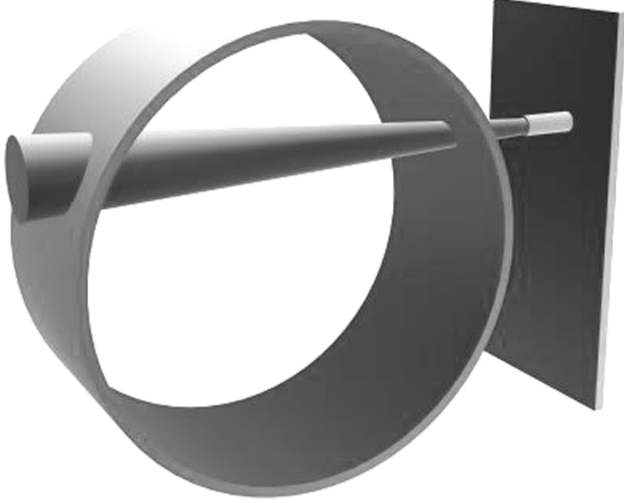


Fig. 4. Backprojection of the cone from a collimator hole through the cylinder.

When we consider the intersection of the cone coming from the collimator hole and the cylinder face, all elements on the cylinder with possible contribution of the radiance to this specific list-mode event are selected, these elements are called scanning points. In every scanning point the emission radiance distribution is parameterized by the angles θ and κ . The face of the cone will put restrictions on these angles since the vector of the escaping radiance has to lay within the cone (image 5). In a first step one has to obtain the area on the cylinder face which is the intersection of the cone and the cylinder. Secondly for each scanning point in this area the restriction on θ and κ have to be applied. This will give the four dimensional region $A_n(\psi, z, \theta, \kappa)$

When we integrate the emission radiance distribution $F(\phi, z, \theta, \kappa)$ over the region $A_n(\phi, z, \theta, \kappa)$, we get the contribution of the emitted photons from the total source distribution into the specific detector location during projection. In the backprojection step, A_n defines the region of the object into which the counts in the detector bin will be backprojected and therefore will depict how the detected photons, for a specific detector location, will contribute to the backprojected image. It is also possible to use an expression for the geometric point response in terms of the autocorrelation of the collimator aperture function for one collimator hole [8]. This operator can be used to calculate the individual voxel contributions. When we do not want

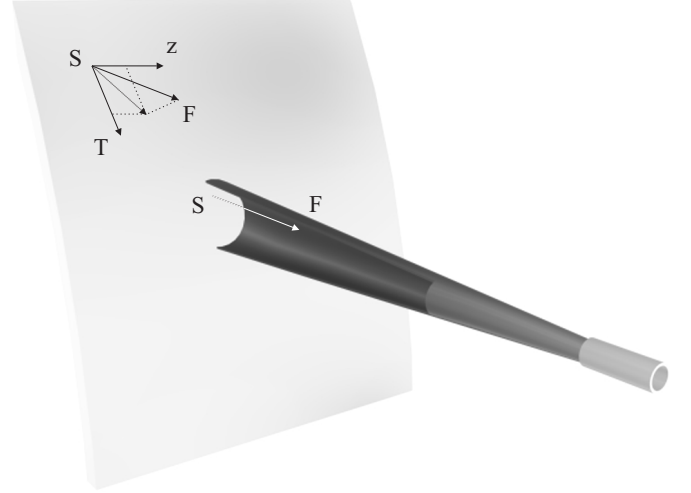


Fig. 5. Selection of the vectors from the emission radiance distribution in the acceptance cone.

to model the effects of attenuation and scatter in the back-projection, but only the distance dependent resolution, we can use the basic collimator aperture function. The effect of the mismatched projector/backprojector pair has to be investigated [9].

C. List-mode reconstruction

Consider a data set of N list-mode events with attributes being the coordinates, gantry angle, energy level, etc. If we want to use the ML algorithm we need to calculate $P_j(l_n)$, for $n = 1, 2, \dots, N$ and $j = 1, 2, \dots, J$, the probability density that an item l_n would occur in the list, given there was an emission of a photon in the j -th voxel.

A list-mode maximum-likelihood reconstruction algorithm for PET was previously developed by Parra et. al. [10], [11] :

$$x_j^{(k+1)} = \frac{1}{N} \cdot \sum_{n=1}^N \frac{P(l_n|j) \cdot x_j^{(k)}}{\sum_{j=1}^J P(l_n|j) \cdot s_j \cdot x_j^{(k)}} \quad (2)$$

In this equation $x_j^{(k)}$ is the expected number of photons emitted from source bin j per unit of time for the k^{th} iteration, and s_j is the sensitivity for that source bin. N is the number of list-mode events. J is the number of source bins.

The nominator in the summation over the list-mode events N is probability density given above. This can be seen as the probability that an emission in voxel j will lead to the detection of the list-mode event l_n . The denominator is the total over all voxel of the probability density functions given the detection of event l_n . When we look at the radiance distribution this will give the probability density functions of photons coming from the source distribution, leaving the intermediate layer in a specific direction. In the previous section we discussed how to restrict the area on the intermediate layer for a given list-mode event. Doing

this we can obtain the contribution of the radiance distribution to a specific event. This is equal to the denominator in equation. The nominator can be calculated from the radiance for a single voxel or by using the collimator aperture function. Therefore, the equation can be rewritten as follows:

$$Y_{jn}^{(k+1)} = \frac{\oint_{A_n} F_j^{(k)}(\phi, z, \theta, \kappa)}{\oint_{A_n} F^{(k)}(\phi, z, \theta, \kappa)} \quad (3)$$

where A_n is the list-mode specific acceptance area. $F_j^{(k)}$ is the radiance distribution for voxel j for the k^{th} estimate, and $F^{(k)}$ is the total radiance distribution for the k^{th} source estimate. Since one list-mode event is the detection of a single photon, the backprojected value is normalized to 1.

$$y_{jn}^{(k+1)} = \frac{Y_{jn}^{(k+1)}}{\sum_{j=1}^J Y_{jn}^{(k+1)}} \quad (4)$$

$$x_j^{(k+1)} = \sum_{n=1}^N y_{jn}^{(k+1)} \quad (5)$$

The algorithm updates the estimate of the source distribution for each list-mode event and sums the individual results to the final new estimate for the source distribution. In this way the integrals can be calculated on the fly and do not have to be stored. The reconstruction starts from a uniform source distribution to calculate the primary radiance. After a run through the list-mode data set, the emission radiance distribution is recalculated and used in the next iteration.

III. RESULTS

Preliminary test of the reconstruction algorithm were performed on a simple three dimensional Gaussian distributed sphere with FWHM of a central cross section equal to 12.5 mm, placed in the center of a 32 cube matrix with voxel size 3,125 mm. List-mode information for this object was derived from Monte-Carlo simulation, where the data was acquired in projections of 512x512 detector bins over 360 angles. A high-resolution parallel-hole collimator was specified, with hole size 1.4 mm, length 27 mm and radius of rotation equal to 112 mm. This results in the maximum diameter of the backprojected cone being 14.4 mm or less than 5 voxels. The initial emission radiance distribution was derived from a uniform cylinder with radius 10 cm within the 32x32x32 matrix. As with the 2D LMIRA, the three dimensional reconstruction is resolving the object over the different iterations. Further study is needed to optimize the reconstruction procedure.

IV. DISCUSSION AND CONCLUSION

In this study we propose an extension of the 2D list-mode reconstruction towards fully three dimensional image reconstruction. Calculating the emission radiance distribution it is possible to incorporate the effects of attenuation and scatter. This can be done by using ray-tracing as

implemented in the 2D LMIRA. A different approach could be using a model based deformation of the radiance based on the attenuation and electron density maps. The calculation of the 4D radiance function is a computational intensive task. In our approach this calculation has to be done once every iteration. The calculation of the intersection of the cone coming from the collimator hole and the cylinder could be used more efficiently to define the voxel within the object which can possibly contribute to the list-mode event. In that way the number of voxel which have to be taken into account in the reconstruction of a single event can be reduced significantly.

ACKNOWLEDGMENTS

This work was supported by "Institute for the Promotion of Innovation by Science and Technology in Flanders" (IWT, Belgium). Rik Van de Walle is a post-doctoral fellow of the Fund for Scientific Research-Flanders (FWO, Belgium). We thank Marconi Medical Systems for their support on the list-acquisition with the Irix gamma camera.

REFERENCES

- [1] AJ Reader, K Erlandsson, and RJ Ott, "Attenuation and scatter correction of list-mode data driven iterative and analytic image reconstruction algorithms for rotating 3D PET systems," *IEEE Transactions on Nuclear Science*, vol. 46, pp. 2218–2226, December 1999.
- [2] SJ Wilderman, WL Rogers, GFKnoll, and EJCngdahl, "Fast algorithm for list mode back-projection of compton scatter camera data," *IEEE Transactions on Nuclear Science*, vol. 45(3), pp. 957–962, 1998.
- [3] L Bouwens, R Van de Walle, J Nuyts, M Koole, Y D'Asseler, S Vandenberghe, RA Dierckx, and I Lemahieu, "Image-correction techniques in spect," *Computerized Medical Imaging and Graphics*, vol. 25, pp. 117–126, March-April 2001.
- [4] L. A. Shepp and Y. Vardi, "Maximum likelihood reconstruction for emission tomography," *IEEE Transactions on Medical Imaging*, vol. 1, pp. 113–122, Oct. 1982.
- [5] K. Lange and R. Carson, "EM reconstruction algorithms for emission and transmission tomography," *J. Comput. Assist. Tomogr.*, vol. 8, pp. 306–316, April 1984.
- [6] L Bouwens, R Van de Walle, H Gifford, MA King, I Lemahieu, and RA Dierckx, "LMIRA: List mode iterative reconstruction algorithm for SPECT," *submitted for publication*, 2001.
- [7] L Bouwens, H Gifford, R Van de Walle, MA King, I Lemahieu, and RA Dierckx, "Resolution recovery for list mode reconstruction in SPECT," *submitted for publication*, 2001.
- [8] GT Gullberg, BM Tsui, CR Crawford, JG Ballard, and JT Haggis, "Estimation of geometrical parameters and collimator evaluation for cone beam tomography," *Medical Physics*, vol. 17(2), pp. 264–272, 1990.
- [9] SJ Glick and EJ Soares, "Noise characteristics of SPECT iterative reconstruction with a mismatched projector-backprojector pair," *IEEE Transactions on Nuclear Science*, vol. 45, pp. 2183–2188, August 1998.
- [10] HH Barrett, T White, and LC Parra, "List-mode likelihood," *Journal of the Optical Society of America A-Optics Image Science and Vision*, vol. 14, pp. 2914–2923, November 1997.
- [11] L. Parra and H.H. Barrett, "List-mode likelihood : EM algorithm and image quality estimation demonstrated on 2-D PET," *IEEE Transactions on Medical Imaging*, vol. 17, pp. 228–235, April 1998.